

ISOTHERMAL OXIDATION BEHAVIOR AND THERMAL SHOCK RESISTANCE OF THREE-KIND Cr COATINGS ON PCrNi3MoVA STEEL

Q. LI^a, M. HU^{b,*}, P. ZHANG^a, C. GUO^b, Q. NIU^a

^a*School of Mechatronic Engineering, North University of China, 3 Xueyuan Road, 030051 Taiyuan, China*

^b*School of Equipment Engineering, Shenyang Ligong University, 6 Nanpingzhong Road, 110159 Shenyang, China*

Isothermal oxidation behavior at 900 °C for 5 h and thermal shock resistance at 900 °C of three-kind Cr coatings prepared by electroplating, magnetron sputtering and multi arc ion plating technologies on PCrNi3MoVA steel were investigated. Micromorphologies of three-kind Cr coatings before and after tests were observed by the scanning electron microscopy and crystallization phase identification was studied by the X-ray diffraction. Oxidation of three-kind Cr coatings showed characteristic morphologies of electroplating Cr coating with microcrack, magnetron sputtering Cr coating with columnar crystal and multi arc ion plating Cr coating with microdroplet during coating preparation were main reasons for different properties. Correspondingly, the failure mechanisms of delamination, through spalling caused by through cracks and through spalling caused by surface spalling of droplet were obtained by thermal shock test. The results indicate that multi arc ion plating, for its property of high temperature resistance, could be a more effective approach to prolong gun barrel life.

(Received February 13, 2020; Accepted July 28, 2020)

Keywords: Isothermal oxidation, Thermal shock, Cr coating, PCrNi3MoVA steel

1. Introduction

Gun barrel life is the key factor restricting the whole performance of gun. During a projectile launch, the inner surface of gun barrel has an approximate temperature of 1100 °C and a pressure of 400 MPa within just a few milliseconds. Such an extreme condition can makes the residual life of the gun barrel to shorten down[1-4]. At present, the electroplating Cr coating, as a cost-effective technology, is commonly applied to prolong the gun barrel life. However, the electroplating Cr coating technology has been eliminated due to its two obvious disadvantages in engineering applications. One is the easy appearance of microcracks on the inner surface of gun barrel, and the other is the risk of potentially carcinogenic substances for Cr 6+ 0. At the same time, the Cr should be still realized as an ideal coating material of gun barrel for its excellence of being high-temperature resistant, wearing resistant and efficient. It may be a feasible method for prolonging the gun barrel life to prepare coating by combining chromium with new coating preparation technology.

As a coating preparation technology, physical vapor deposition (PVD) is widely employed in many industrial fields. Magnetron sputtering and multi arc ion plating, as two important physical vapor deposition (PVD) technologies, have the advantages of high deposition rate, convenient parameters control, high kinetic energy and environmentally friendly, compared with other deposition methods[6-8]. These advantages would be able to achieve better Cr coatings than electroplating technology. Up to now, some researches about coating preparations on the surface of gun bore or gun steel (PCrNi3MoVA steel) by magnetron sputtering and multi arc ion plating in PVD have been done. However, these researches have deposited TantalumO and TiAlN0 instead of Cr Coatings, and more attention is paid to mechanical properties such as adhesion and friction and wear. Erosion as the primary cause of gun barrel failure has not received enough attention, although the adhesion and wear properties are also important. Many details of the erosion process

* Corresponding author: minghu.sylu@163.com

on the surface of gun barrel remain subjects of debate, it is generally accepted that the major contributors to erosion damage are thermal effects and chemical attack by propellant gases. Short pulses of high thermal energy during firings and the resulting temperature accumulation will produce deleterious thermal effects including thermal and transformational stresses, cracks and even melting⁰. In our previous work, crystallographic orientation and oxidation behaviour of Cr films deposited on gun steel via multi arc ion plating are significantly affected by ion bombardment energy, and it is found that self-ion bombardment can be an effective approach to improve the oxidation resistance of gun steel⁰. However, this result lacks comparison with magnetron sputtering Cr coating, including electroplating Cr coating.

Hence, in this study, the corresponding isothermal oxidation and thermal shock tests were designed to simulate erosion conditions during firing. we investigated isothermal oxidation behavior and thermal shock resistance of magnetron sputtering Cr coating and multi arc ion plating Cr coating contracting to electroplating Cr coating on PCrNi3MoV steel. The microstructure of three-kind Cr coatings deposited was characterized. The oxidation and thermal shock resistant behaviors of three-kind Cr coatings and failure mechanism of three-kind Cr coatings at high temperatures at 900 °C were investigated by observing microstructure changes and coatings morphologies.

2. Experimental

2.1. Materials

A high strength steel used for gun barrel PCrNi3MoV (Changjue Metals Co., Ltd., Kunshan, China) was employed as the substrate for the deposition of pure Cr coatings. The nominal chemical compositions of the substrate steel are listed in Table 1.

Table 1. Chemical composition of the gun steel.

Elements	C	Mn	Si	Cr	Ni	Mo	V	S	P	Fe
wt.%	0.40	0.41	0.25	1.28	3.14	0.37	0.20	0.001	0.012	In balance

Due to the different requirements of the three-kind Cr coatings preparation equipment, the specific dimensions of each specimen are slightly different. The electroplating Cr specimens of 15 mm × 10 mm × 3 mm in size were cut from a plate by a spark discharge machine, and the magnetron sputtering Cr specimens were 15 mm × 15 mm × 3 mm, the multi arc ion plating Cr specimens were 20 mm × 10 mm × 3 mm. All of the specimen surfaces were ground on 1000# SiC paper. Prior to the coating deposition, the specimens were rinsed in ethanol for 5 min with the assistance of ultrasonic to eliminate contaminations.

2.2. Coatings preparation

2.2.1 Electroplating Cr coating preparation

The preparation of electroplating Cr coating consults electroplating method, which is similar to the electroplating deposition parameters of the gun in service so as to make a more objective comparison. The plating bath composition and main deposition parameters of electroplating Cr coating are listed in Table 2.

Table 2. Plating bath composition and main deposition parameters.

Plating bath composition and deposition parameters	Value
CrO ₃	250 g/L
H ₂ SO ₄	2.5 g/L
Deposition voltage	> 12V
Deposition temperature	60°C
Deposition current	50 A
Deposition time	2 h
Current density	20 A/dm ²

2.2.2 Magnetron sputtering Cr coating preparation

The pure Cr coatings were prepared in an MS machine (QHV-JGP400B II, Sky technology development CO., LTD. Shenyang, China). Prior to the Cr coating deposition, the inner surface was firstly polished with 600# SiC paper as well as dusted with a vacuum cleaner, and then wiped with the absorbent cotton soaked in anhydrous ethanol. Finally, glow cleaning of gun steel lasted for 30 minutes. The purity of Cr target is 99.95 wt % (Industry pure Cr containing about 0.05 wt % Fe, Jingmaiyan Material Technology Co., Ltd., Beijing, China). The process parameters of Cr coating deposited by magnetron sputtering are listed in Table 3.

Table 3. Process parameters of Cr coating deposited by magnetron sputtering.

Deposition parameters	Value
Deposition current	0.3 A
Deposition voltage	360 V
Negative bias voltage	100 V
Substrate temperature	350°C
Partial pressure of Ar gas	0.5 Pa
Rotation rate	30 r/min
Power	100 W
Deposition time	10 h

2.2.3 Multi arc ion plating Cr coating preparation

The pure Cr coatings were prepared in an AIP machine (DH-7, Beiyu vacuum technology, Shenyang, China) with water-cooled cylinder vacuum chamber. The chamber size is about 1.2 m in diameter and 1.2 m height. Prior to the Cr coating deposition, the vacuum chamber was evacuated to about 6×10^{-3} Pa as pumped by a combination of an oil diffusion pump and a rotary pump. Prior to arc ignition, specimens were cleaned by Ar⁺ bombardment for 10 min with the substrate bias voltage of -900 V at 20% in duty cycle. To measure the temperature of the specimens, type-K thermocouples were welded on the back side of the specimens. The measured temperature of the specimens during deposition varied between 200–300°C. All of the specimen surfaces were ground on 1000# SiC paper. Prior to the coating deposition, the specimens were rinsed in ethanol for 5 min with the assistance of ultrasonic to eliminate contaminations. The purity of Cr target is 99.9 wt % (Industry pure Cr containing about 0.1 wt % Fe, Jingcheng Titanium Co., Ltd., Baoji, China). The process parameters of Cr coating deposited by multi arc ion plating are listed in Table 4.

Table 4. Process parameters of Cr coating deposited by multi arc ion plating.

Deposition parameters	Value
Vacuum degree	6×10^{-3} Pa
Target substrate distance	200 mm
Rotation rate	10 r/min
Vacuum chamber temperature	150-250°C
Partial pressure of Ar gas	0.1 Pa
substrate bias voltage	-50 V
Deposition time	5 h

2.3. Characterization methods

In this work, X-ray diffraction and Scanning electron microscopy were used to study crystallization phase identification and observe micromorphologies in isothermal oxidation test and thermal shock test. X-ray diffraction (XRD, X' Pert PRO, PANalytical Co., Almelo, the Netherlands, Cu K α radiation at 40 kV) was employed for phase identification of the as-prepared Cr coatings before and after oxidation. During XRD detection, the specimen was kept static as the point of origin, while the incident X-ray and the detector rotated simultaneously around the origin in opposite direction. The included angle between the incident X-ray and the normal direction of the specimen varied between 10°–45°. In the meantime, the detector rotated symmetrically around the origin. Hence, the detected range of 2 θ is 20°–90°. Scanning electron microscopy (SEM, InspectF 50, FEI Co., Hillsboro, OR) and energy dispersive spectroscopy (EDS, INCA, X-Max, Oxford instruments Co., Oxford, U.K.) were used for the observation of surface morphology and cross-section as well as the analysis of the composition of the coatings thermal shock and surface oxide scales.

Isothermal oxidation tests were conducted at 900 °C in air in a muffle furnace. Each specimen was heated for 5 h at 900 °C. Such short-term oxidation is designed according to the application of the steel, due to that the gun barrel subjects to high temperatures for only milliseconds during each firing. The overall exposure time of the steel at high temperatures would be seldom longer than 5 h. For the oxidation tests, specimens were directly put into the furnace which had been preheated to 900 °C in advance. It usually took one or two minutes to raise the temperature to 900°C for the small specimen. After oxidation for 5 h, the specimens were taken out of the furnace to be cooled in air. Electroless nickel plating was introduced to coat the specimens after oxidation to assist with analyzing the oxide scales in cross-sectional view[12,13]. The SEM observation and EDS analysis of the surface oxide scale were carried out on the other oxidized specimens in parallel, which were not treated by the Ni plating after oxidation. However, to improve the electric conductivity of the surface, C-coatings were coated by evaporation of carbon threads for 3–5 s in vacuum on the oxidized specimen prior to SEM observation.

Thermal shock tests were conducted between 900 °C and room temperature in air in a muffle furnace. After being maintained in a muffle furnace at 900 °C for 10 min, the three-kind Cr coating specimens were taken out immediately and immersed into water with room temperature. After that, the three-kind Cr coatings specimens were put into the furnace for the next cycle, and the thermal shock test would be terminated when the failure phenomena such as crack and peeling occur. The SEM observation of the surface failure morphology of thermal shock specimens was carried out. Similarly, to improve the electric conductivity of the surface, C-coatings were coated by evaporation of carbon threads for 3–5 s in vacuum on the thermal shock specimens prior to SEM observation.

3. Results and discussions

3.1. Microstructure of three-kind Cr coatings

Fig. 1 shows the SEM images of the surface morphologies and cross-sections of the three-kind Cr coatings deposited by electroplating, magnetron sputtering and multi arc ion plating.

According to the surface morphology, the characteristic morphologies of the three-kind Cr coatings are clearly different, although all three coatings are composed of pure Cr. Intersecting microcracks, which is difficult to avoid in the preparation of Cr coatings by electroplating technology, are observed in the surface of electroplating Cr coating. The microcracks are closely related with H^+ produced during preparation. Cr is produced by decomposition of CrH at the cathode with the formation of hydrogen. Hexagonal CrH is decomposed into Cr with bcc lattice is a contributor to the internal stress increase. Meanwhile, with the increase of coating thickness, cracks are produced to release part of internal stress. The cross-sectional images (Fig. 1(b)) of the electroplating Cr coating shows almost straight surface profiles, which further confirms the formation of the much smoother surfaces. Microcracks perpendicular to the coating surface are also observed like the Fig. 1(a). Fig. 1(c-d) shows the SEM images of the surface morphology and cross-section of the magnetron sputtering Cr coating. The surface of magnetron sputtering Cr coating is smooth and compact without obvious defects, but the microcracks and small pores are observed in the corresponding cross-section because of the existence of columnar defects. The existence of small pores indicates that the bonding strength of magnetron sputtering Cr coating with gun steel substrate is slightly insufficient. Fig. 1(e-f) shows the SEM images of the surface morphology and cross-section of the multi arc ion plating Cr coating. Microdroplets which are always present in AIP depositions can be clearly identified on the surfaces of Cr coatings obtained[16,17]. The interface between multi arc ion plating Cr coating and gun steel substrate is very straight. There are no obvious pores or microcracks in the multi arc ion plating Cr coating. As we know, the flat and compact surface can often show better property, when the coating is eroded or worn. For the microstructure of three-kind Cr coatings, it is found that microcrack, columnar crystal and microdroplet are the characteristic morphologies, corresponding to electroplating, magnetron sputtering and multi arc ion plating.

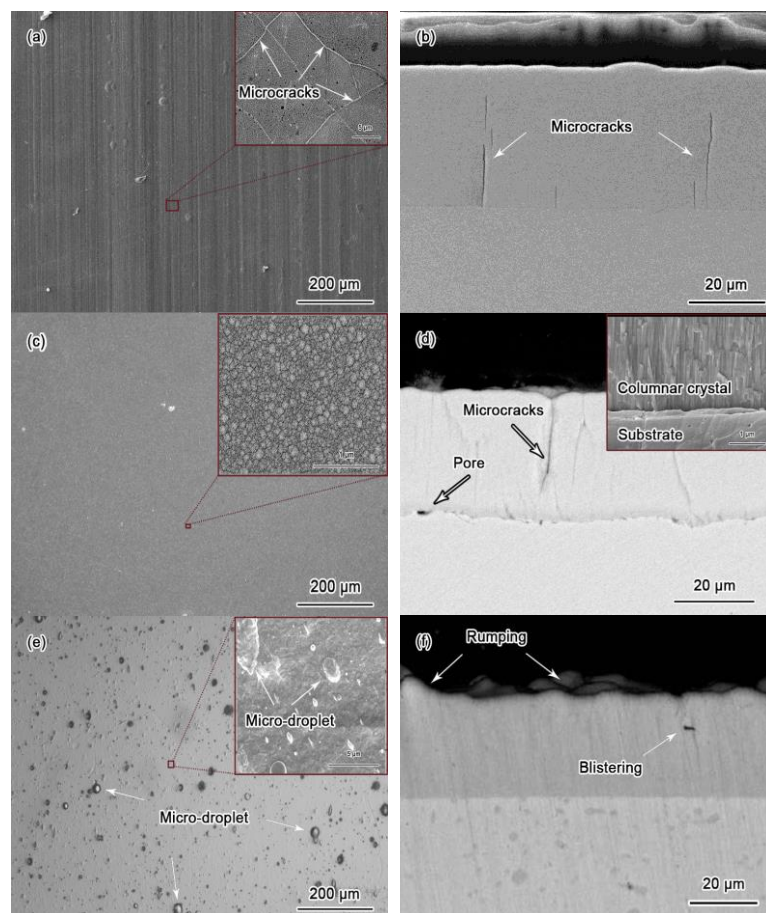


Fig. 1. SEM images of the surfaces of the as-prepared Cr coatings deposited: (a) electroplating, (c) magnetron sputtering and (e) multi arc ion plating, and the corresponding cross-sections (b) electroplating, (d) magnetron sputtering and (f) multi arc ion plating.

Fig. 2 shows the XRD patterns of the pure Cr coatings deposited by electroplating, magnetron sputtering and multi arc ion plating. Three major diffraction peaks of (110), (200) and (211) of Cr can be clearly identified in the patterns. The phenomenon that only Cr can be identified indicates that the X-ray did not penetrate through each of the three Cr coatings. Hence, the XRD patterns are not affected by the slight variation of thickness of the Cr coatings. No peak widening is observed. However, the trend of strong crystallographic orientation can be observed between three-kind Cr coatings. All the three-kind Cr coatings are bcc α phase structure, with the crystal size of electroplating Cr coating being about 28 nm, that of magnetron sputtering Cr coating being about 20 nm, and that of multi arc ion plating Cr coating being about 15 nm. The coating preparation method has no effect on the phase of Cr coating, but which can affect the crystallographic orientation and crystal size.

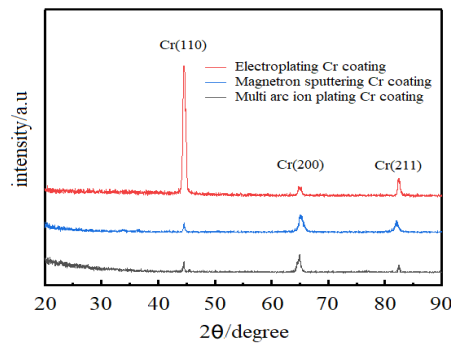


Fig. 2. XRD patterns of the as-prepared Cr coatings deposited under electroplating, magnetron sputtering and multi arc ion plating.

3.2. Isothermal oxidation behavior of three-kind Cr coatings

Fig. 3 shows the SEM images of the surface and corresponding magnified morphologies of the three-kind Cr coatings after oxidation in air at 900 °C for 5 h. Fig. 3(a-b) shows the SEM image of the surface and corresponding magnified morphology of the electroplating Cr coating after oxidation in air at 900 °C for 5 h. The oxide scale grown on the electroplating Cr coating shows a large number of intersecting microcracks have been formed and developed into net cracks gradually. Except for the surface, Cr_2O_3 scale is also found in crack gap by the EDS. The corresponding cross-section of Cr_2O_3 scale in crack gap shows the oxidation behavior has spread through the electroplating Cr coating to the gun steel substrate. A natural channel for oxidation behavior is provided by microcracks which perpendicular to the coating surface especially. Crack gaps are filled with the growing Cr_2O_3 scale, which forms rumpling by jacking up Cr_2O_3 scale on the surface of the electroplating Cr coating. This phenomenon means that the friction and wear resistance, corrosion resistance and erosion resistance of the electroplating Cr coating will be reduced seriously. Fig. 3(c-d) shows the SEM image of the surface and corresponding magnified morphology of the magnetron sputtering Cr coating after oxidation in air at 900 °C for 5 h. The oxide scale grown on the magnetron sputtering Cr coating shows some spalling zones on the surface of Cr_2O_3 scale. A porous Cr_2O_3 scale of approximately 2 μm in thickness grown on the surface of magnetron sputtering Cr coating. The magnified spalling zone (Fig. 3(d)) shows jagged spalling edge, the uncovered part is proved to be magnetron sputtering Cr coating without protection of Cr_2O_3 scale by the EDS. Many microholes which can destroy structural stability of magnetron sputtering Cr coating are observed on the surface of magnetron sputtering Cr coating after peeling off. The exchange of materials and energy between internal and external can be realized through these microholes, and it is easy to develop into cracks. Fig. 3(e-f) shows the SEM image of the surface and corresponding magnified morphology of the multi arc ion plating Cr coating after oxidation in air at 900 °C for 5 h. The oxide scale grown on the multi arc ion plating Cr coating shows successive and dense Cr_2O_3 scale is formed on the surface without microcracks and partial spalling. The magnified zone (Fig. 3(f)) shows microdroplets that will be an unstable

factor for spalling and cracking of the multi arc ion plating Cr coating still exist and are covered under the Cr_2O_3 scale. Furthermore, the thickness of Cr_2O_3 scale grown on the surface of multi arc ion plating Cr coating is about $1.7\ \mu\text{m}$, slightly thinner than the thickness of magnetron sputtering Cr coating. This result may benefit from the smaller crystal size and denser microstructure. According to the oxidation morphologies, it is found that oxide scales closely related to the characteristic morphologies of the three-kind coatings.

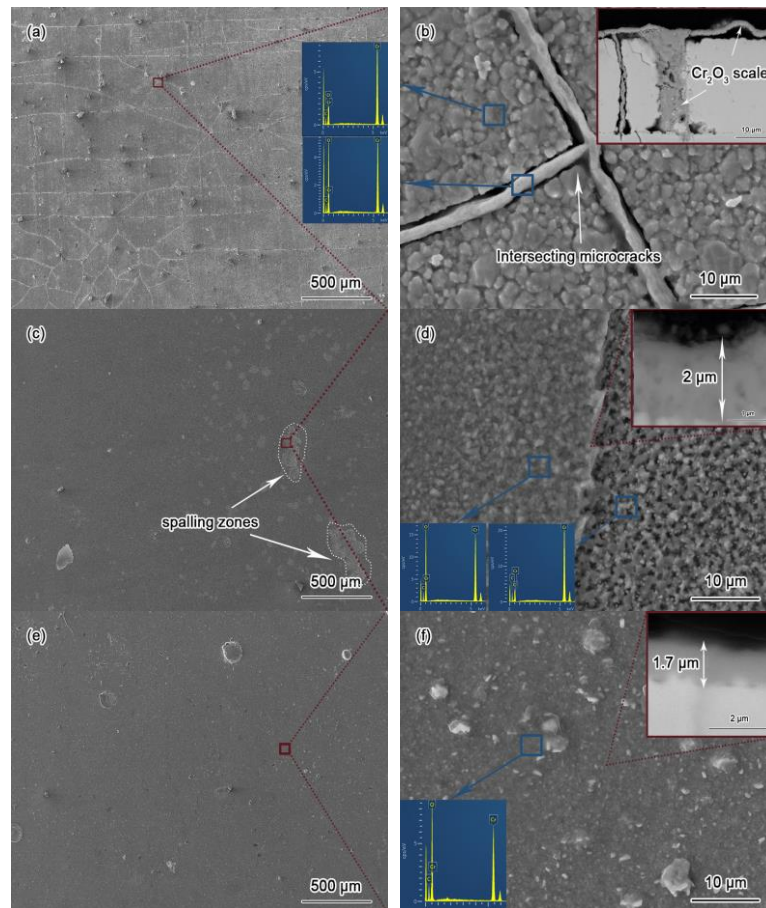


Fig. 3. SEM images of the surfaces of the three-kind Cr coatings after oxidation in air at 900°C for 5 h: (a) electroplating, (c) magnetron sputtering and (e) multi arc ion plating, and the corresponding magnified images (b) electroplating, (d) magnetron sputtering and (f) multi arc ion plating.

Fig. 4 shows the XRD patterns of three-kind Cr coatings after oxidation in air at 900°C for 5 h. According to the patterns, Cr_2O_3 scale has been formed on the three-kind Cr coatings during oxidation, and the mainly diffraction peaks of multi arc ion plating Cr coating are Cr_2O_3 , Cr and FeCr alloy phases, compared with the pure Cr_2O_3 diffraction peaks of the magnetron sputtering Cr coating and electroplating Cr coating. The newly emerged FeCr alloy phase was not detected before the oxidation, indicating the occurrence of interdiffusion between the multi arc ion plating Cr coating and the gun steel substrate during oxidation 0.

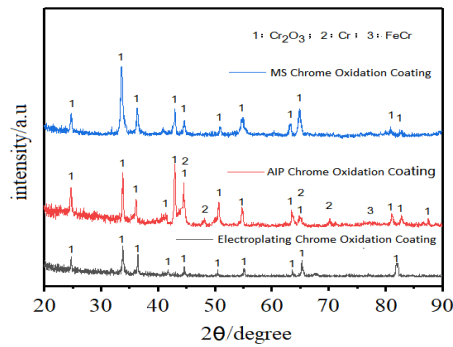


Fig. 4. XRD patterns of three-kind Cr Coatings after oxidation in air at 900 °C for 5 h.

3.3. Thermal shock resistance of three-kind Cr coatings

Fig. 5 shows the SEM images of the surface and corresponding magnified morphologies of the three-kind Cr coatings after several thermal shock cycles at 900°C for 10 min. In order to better show the failure characteristics of three-kind Cr coatings, surface morphologies are shown respectively for electroplating Cr coating after 5 thermal shock failure cycles, the magnetron sputtering Cr coating after 18 thermal shock failure cycles and multi arc ion plating Cr coating after 18 thermal shock failure cycles. According to the surface morphology, the different failure modes of three-kind Cr coatings are shown clearly. Similar to the oxidation morphology (Fig. 3(a)), there are many microcracks on the surface of electroplating Cr coating after 5 thermal shock cycles. As shown in Fig. 5(b), a microcrack with a width of about 20 μm penetrates into the electroplating Cr coating, and the crack gap can be seen obviously. At the same time, it is found that delamination has occurred along the growth trend of net cracks. This phenomenon means that the electroplating Cr coating can no longer provide protection for gun steel substrate, and the number of thermal shock failures cycles is 5. Fig. 5(c-d) shows the surface morphologies of magnetron sputtering Cr coating after 18 thermal shock failure cycles. Distinguishing from failure mode of electroplating Cr coating, delamination do not occur on the surface of magnetron sputtering coating, instead through microcracks with the width of about 20 μm. Such through microcracks could be seen in the coating with rapid temperature change 0. Many properties just as friction and wear resistance, corrosion resistance and erosion resistance of the magnetron sputtering coating will be greatly affected, especially when a crack completely penetrates the coating. Under the same thermal shock failure cycles, neither delaminations nor microcracks are found on the surface of multi arc ion plating Cr coating, which is comparatively complete without obvious defects (Fig. 5(e-f)). Careful observation shows that surface spalling has occurred due to the spalling of microdroplets on the surface of multi arc ion plating Cr coating during the thermal shock failure cycles. It means that the microdroplet spalling from the surface of multi arc ion plating Cr coating is responsible for surface spalling. With the spalling aggravating, surface spalling will develop into pits spalling, which is the key factor contributing to multi arc ion plating Cr coating failure. Thermal shock resistance of three-kind Cr coatings is based on the respective oxidation behavior.

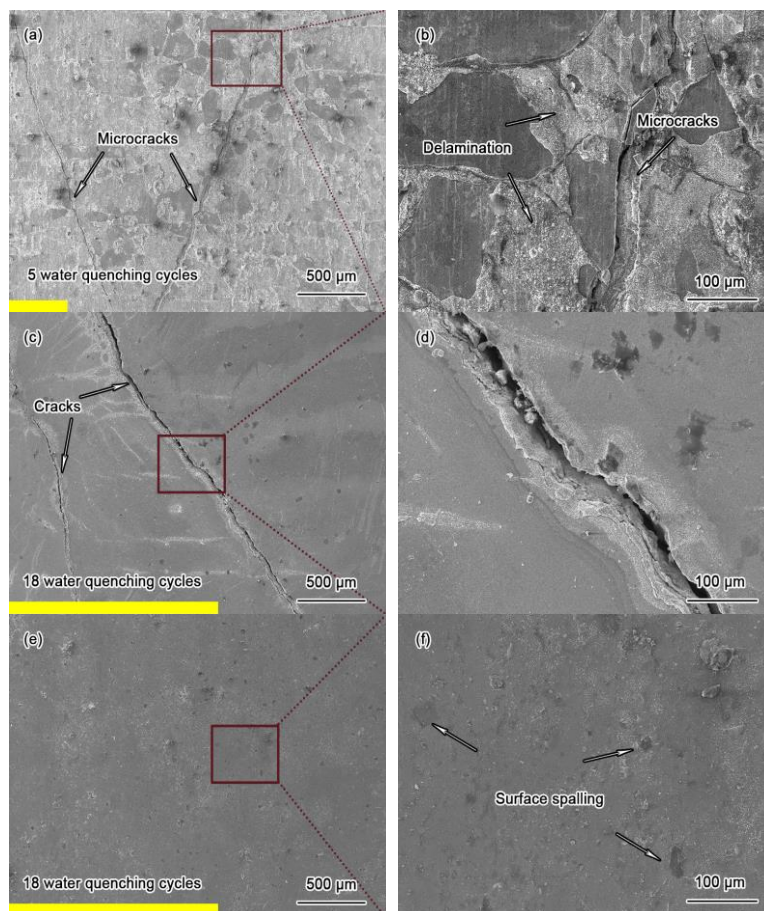


Fig. 5. SEM images of the surfaces of the three-kind Cr coatings after several thermal shock cycles at 900 °C (a) electroplating, (c) magnetron sputtering and (e) multi arc ion plating, and the corresponding magnified images (b) electroplating, (d) magnetron sputtering and (f) multi arc ion plating.

3.4. Oxidation and thermal shock failure mechanism of three-kind Cr coatings

The results of the isothermal oxidation test of three-kind Cr coatings in air at 900 °C for 5 h indicate that protective dense oxide scales have been formed on all the surface of three-kind Cr coatings, but the oxidation degree and characteristics are different obviously. The surface of electroplating Cr coating fails to form a complete and continuous oxide scale, due to the existence of microcracks. The oxide scales are divided by the net microcrack and oxidized further inside the electroplating Cr coating. Some studies have shown that changing current density and deposition temperature can effectively reduce microcracks density, but it needs to be mentioned that this reduction is accomplished at the sacrifice of surface hardness and cathodic current efficiency, respectively 0. It is difficult to reduce microcracks while ensuring properties of electroplating Cr coating. The surfaces of magnetron sputtering and multi arc ion plating coatings have formed dense oxide scales with different thickness, although there is a little spalling on the surface of magnetron sputtering Cr coating. As shown in Fig. 3(f), the reason why the multi arc ion plating oxide scale is complete is that the microdroplets are wrapped under the oxide scale without peeling off. As is known to all, dense oxide scale is a good protective layer for Cr coating. The oxide scale relatively complete without spalling can provide better protection for the Cr coating. Furthermore, oxide scale with 1.7 μm thickness of multi arc ion plating Cr coating is thinner than 2 μm thickness of magnetron sputtering Cr coating. The smaller crystal size of multi arc ion plating Cr coating is beneficial to decrease growth rate of Cr₂O₃ scale. Besides, the crystal size is also related to the formation of microcrack. The relationship between crystal size and microcrack can be given

as 0:

$$\varepsilon = \frac{\sigma\Omega}{d^2kT} \left(B_1D_V + \frac{B\delta D_B}{d} \right) \quad (1)$$

where ε is the deformation rate, σ is the tensile stress, Ω is the atomic volume, d is the average crystal size, B is numerical constants, D_V and D_B are the volume and boundary diffusivities, kT has the usual meaning and δ is the thickness of the boundaries. For the same Cr material, it can be seen from the Eq. (1) that the coating with smaller crystal size can produce larger deformation rate, and then reduce the microcrack growth rate. As analyzed in this paper, the reduction of microcrack number is beneficial to the improvement of the oxidation resistance of Cr coating. Except the influence of crystal size, the main factor for the difference of oxidation resistance of three-kind Cr coatings are the typical characteristic morphologies during coating preparation: microcrack, columnar crystal and microdroplet.

For the thermal shock test of three-kind Cr coatings in air at 900 °C for 10 min by water quenching, the results show a good agreement with that of isothermal oxidation test. From Fig. 3(a-b) to Fig. 5(a-b), some microcracks would turn to large cracks with the test going on because of the accumulation of residual stress. The large cracks is helpful for the oxygen diffusion and would lead to the detachment of the coating from the substrate. From Fig. 3(c-d) to Fig. 5(c-d), the gaps between columnar crystals of magnetron sputtering Cr coating are easy to serve as the release outlet of residual stress, which leads to the form cracks causing oxide scale peeling and coating failure. From Fig. 3(e-f) to Fig. 5(e-f), the microdroplets occur surface spalling so as to release residual stress and prevent crack growth. The three-kind Cr coatings show different thermal shock failure modes, which can be explained by residual stress. The coating residual stress can be divided into three parts[23,24]:

$$\sigma_c = \sigma_g + \sigma_a + \sigma_t \quad (2)$$

where σ_g is the growth stress, σ_a is the fatigue stress and σ_t is the thermal mismatch stress. The growth stress originates from deposition process, which is influenced by the deposition parameters. The fatigue stress is affected by such factors as phase transformation, oxidation and chemical reactions. The thermal mismatch stress originates from the difference between the CTEs of the substrate and the coating **Error! Reference source not found.**

In this work, the thermal mismatch stress has no obvious difference for the three-kind Cr coatings, due to the same coating material. It can't show the key effect on the thermal shock resistance and the service life of the coating. For the fatigue stress, It also has less effect without phase transformation or chemical reaction inside the three-kind Cr coatings. Therefore, the growth stress of three-kind Cr coatings plays the critical role in the accumulation of residual stress. The residual stress of electroplating Cr coating is significantly higher than that of magnetron sputtering and multi arc ion plating Cr coatings, for the volume change during the decomposition of hexagonal CrH into Cr with bcc lattice can arouse microcracks and peeling off. This view can also be confirmed by Fig. 3(a-b) and Fig. 5(a-b), and the failure mechanism of electroplating Cr coating is delamination along the growth trend of net cracks. For magnetron sputtering Cr coating, the gaps between columnar crystals is a good way to release residual stress. It is also a reasonable explanation that magnetron sputtering Cr coating has more thermal shock times than electroplating Cr coating. The failure mechanism of magnetron sputtering Cr coating is the through microcracks caused by the gaps between columnar crystals develop into large cracks. For multi arc ion plating Cr coating, microcracks were still not observed on or in multi arc ion plating Cr coating except for surface spalling caused by microdroplets, until the end of 18 thermal shock cycles. This is because microdroplet can release residual stress and prevent crack growth. This phenomenon also explains why multi arc ion plating Cr coating is less prone to occur microcracks compared to the other two Cr coatings 0. Through large cracks of multi arc ion plating Cr coating causing coating failure will

occur when the microdroplet is unable to release the accumulated residual stress after 21 thermal shock cycles. Soon afterwards, the multi arc ion plating Cr coating near the through large cracks are peeled off intensively. Hence, the failure mechanism of multi arc ion plating Cr coating is that the through large cracks are caused by microdroplets peeling off.

Isothermal oxidation behavior and thermal shock resistance are affected by the characteristic morphologies of three-kind Cr coatings. The thermal shock failure mechanisms based on characteristic morphologies are the continuation of oxidation behavior. The thermal shock failure mechanisms of three-kind Cr coatings can be proposed as schematically illustrated in Fig. 6.

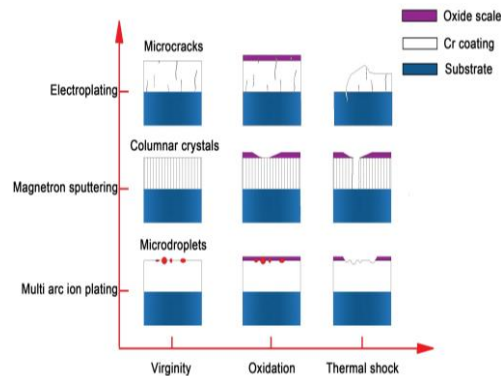


Fig. 6. Schematic illustration of characteristic morphologies and failure mechanisms for three-kind Cr coatings.

4. Conclusions

Three-kind of Cr coatings were prepared by electroplating, magnetron sputtering and multi arc ion plating technologies on the surface of PCrNi3MoVA steel. The isothermal oxidation behavior and thermal shock resistance were studied. This work can enrich the fundamental research of gun barrel life and help to improve the understanding of coating failure mechanism. The following conclusions can be drawn:

(1) Oxidation behavior and thermal shock resistance differences of three-kind Cr coatings mainly come from the typically characteristic morphologies during coating preparation: microcrack, columnar crystal and microdroplet.

(2) Oxidation behavior: microcracks in electroplating Cr coating lead to failure to form a complete oxide scale. Columnar crystals in magnetron sputtering Cr coating may occur oxide scale peeling off. Microdroplets in multi arc ion plating Cr coating is likely to occur surface spalling.

(3) The thermal shock failure mechanisms: delamination for electroplating Cr coating, through spalling caused by through cracks for magnetron sputtering Cr coating, through spalling caused by surface spalling for multi arc ion plating Cr coating. Multi arc ion plating Cr coating shows better oxidation resistance and thermal shock resistance, it could be a more effective approach to prolong gun barrel life.

References

- [1] X. Men, F. Tao, L. Gan, et al., Surf. Coat. Technol. **372**, 369 (2019).
- [2] A. A. Putti, M. R. Chopade, P. E. Chaudhari, International Journal of Current Engineering and Technology **4**, 231 (2016).
- [3] I. Ahmad, Prog. Astronaut. Aeronaut **109**, 311 (1988).
- [4] B. Lawton, Wear **251**, 827 (2001).

- [5] M. Hu, M. Shen, Z. Liu et al., *Corros. Sci.* **143**, 212 (2018).
- [6] G. Bräuer, B. Szyszka, M. Vergöhl, R. Bandorf, *Vacuum* **84**(12), 1354 (2010).
- [7] F. Ali, M. Mehmood, A. M. Qasim et al., *Thin Solid Films* **564**, 277 (2014).
- [8] L. Wang, S. Zhang, Z. Chen et al., *Applied Surface Science* **258**(1), 3629 (2012).
- [9] G. N. Vigilante, C. P. Mulligan, *Materials and Manufacturing Processes* **21**(6), 621 (2006).
- [10] J. Zhang, C. Guo, G. Zhang et al., *Acta Armamentarii* **32**, 697(2011).
- [11] P. J. Cote, M. E. Todaro, G. Kendall, M. Witherell, *Surf. Coat. Technol.* **163-164**, 478 (2003).
- [12] M. Shen, P. Zhao, Y. Gu et al., *Corros. Sci.* **94**, 294 (2015).
- [13] H. Ashassi-Sorkhabi, M. Eshaghi, *Corros. Sci.* **77**, 185 (2013).
- [14] H. E. Townsend, *Corrosion*. **37**(2), 115 (1981).
- [15] A. Misra, S. Fayeulle, H. Kung et al., *Beam Interactions with Materials and Atoms* **148**(1-4), 211 (1999).
- [16] M. Zhang, M. Shen, L. Xin et al., *Corros. Sci.* **112**, 36 (2016).
- [17] P. Zhao, M. Shen, Y. Gu et al., *Surf. Coat. Technol.* **281**, 44 (2015).
- [18] E. Tomanik, M. E. Mansori, R. Souza et al., *Tribol. Int.* **120**, 547 (2018).
- [19] Z. Dong, X. Peng, Z. Guo et al., *Corros. Sci.* **77**, 113 (2013).
- [20] C. Fan, B. Zou, L. Zhu et al., *Materials & Design* **116**, 261 (2017).
- [21] J. G. Zheng, X. D. Zuo, C. W. Wu et al., *Optoelectron. Adv. Mat.* **10**(1), 123 (2016).
- [22] J. Karch, R. Birringer, H. Gleiter, *Nature* **330**, 556 (1987).
- [23] W. Fan, B. Zou, C. Fan et al., *Ceram. Int.* **43**(1), 392 (2017).
- [24] P. Bengtsson, C. Person, *Surf. Coat. Technol.* **92**(1-2), 78 (1997).
- [25] G. W. McClure, *J. Appl. Phys.* **45**, 2078 (1974).